

COMPUTER ANALYSIS AND FORECASTING IN THE TROPICS*

HAROLD A. BEDIENT

Lt. Col., U.S. Air Force
and

JOSEPH VEDERMAN

U.S. Weather Bureau, Honolulu, Hawaii

ABSTRACT

Computer-prepared analyses of the upper-air wind field are being made for several levels for the tropical Pacific Ocean area of both the Northern and Southern Hemispheres. Computer analyses compare favorably with conventional analyses. The availability and accuracy of wind reports from aircraft are discussed. Some details of the IBM 704 tropical analysis program are pointed out.

Computer analyses are used in a statistical wind-forecasting technique for the Tropics. Verification shows that the statistical forecasts are about as good as those prepared by conventional methods.

Experiments aimed at objectively deriving a stream function from observed winds are described and the results discussed.

1. INTRODUCTION

For the past 12 months, July 1963 through June 1964, inclusive, daily objective analyses have been prepared for the 700, 500, 300, and 200-mb. wind fields for the tropical Pacific Ocean area. These analyses have been made with a high-speed electronic computer (IBM 704) by a U.S. Air Force, Navy, and Weather Bureau group in Honolulu, Hawaii. The area analyzed includes both the Northern and Southern Hemisphere Tropics of the Pacific. This is the first time tropical analyses have been prepared routinely by computer for so long a period and for so large an area.

The objectively analyzed winds have been used to prepare barotropic forecasts and are being used as one parameter in a statistical wind-forecasting method.

The purpose of this paper is to discuss the procedures used, show some examples of tropical computer analyses, and point out some of the problems encountered.

One point should be made at the outset. The day is gone when tropical meteorologists in the Pacific could point to the small amount of upper-air data available to them as compared with the much larger amount in middle latitudes. The fact is that extratropical meteorologists are becoming envious of the large number of upper-air reports of winds, temperatures, and weather available in the tropical Pacific. An example of a 250-mb. chart prepared in Honolulu is shown in figure 1. Note that more reports exist in the Tropics than in middle latitudes of the north Pacific—to say nothing of the rarity of reports from middle latitudes of the south Pacific.

The area covered by our computer analysis extends from 115°W. westward, across the Pacific Ocean, to 100°E. and from 37°N. to 24°S. The distance between grid points is 5° longitude at the equator (300 n. mi.). Figure 2 shows the network of grid points on a Mercator projection map. Also shown are the areas covered by the analysis “scans” discussed in the next section.

2. TECHNIQUE OF ANALYSIS

Most computer wind-analysis schemes now in use take into account both the observed heights and winds on appropriate constant-pressure surfaces. However, it is generally considered that height gradients are poorly related to winds in the Tropics [1]. For that reason our analysis method makes no use of the reported heights of constant-pressure surfaces whether obtained from radiosondes or aircraft; it uses winds only.

Reed [2] and others have recently raised some doubts about the alleged failure of the geostrophic relation in the Tropics. Should further study reveal that the geostrophic approximation is not as poor as now thought, an attempt will be made to use the heights of constant-pressure surfaces as well as the winds in the analysis program.

The observed winds are from three sources: pibals, rawins, and aircraft. Perhaps a word should be said about the aircraft reports. For years some forecasters have been skeptical about the accuracy of aircraft wind reports. We do not share that skepticism. Our experience in the Pacific has been that wind reports from aircraft are of excellent quality, even if occasionally in error. The introduction of Doppler wind-measuring

*Revised version of a paper delivered at the Symposium on Tropical Meteorology held in New Zealand in November 1963.

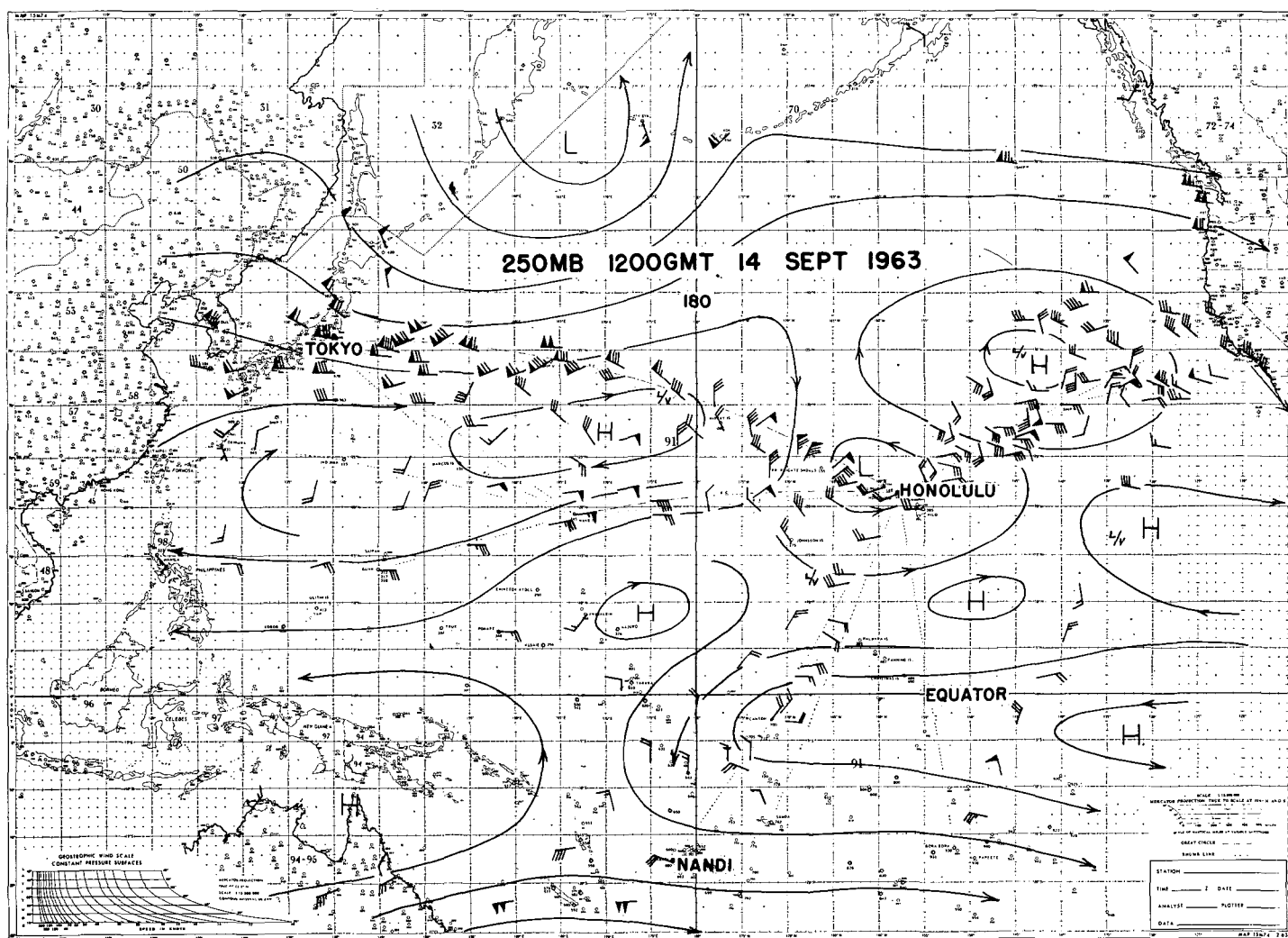


FIGURE 1.—250-mb. chart for 1200 GMT September 14, 1963. In addition to wind reports from pibal and radiosonde stations this chart contains 125 wind reports from jet aircraft.

equipment in some commercial aircraft has further increased our confidence in the reported winds.

Following Berghthorsson and Döös [3] and Cressman [4] we begin the tropical wind analysis with a first approximation to the wind at each grid point. The latest available analysis is used for the first approximation; for example, the first approximation to the 1200 GMT analysis is the preceding 0000 GMT analysis.

The first-approximation winds at the grid points are then corrected by making use of the observed wind reports. The correction formula is

$$\begin{aligned} C_u &= -W(u_i - u) \\ C_v &= -W(v_i - v) \end{aligned} \quad (1)$$

where C is the correction computed for a nearby grid point, u and v are the observed wind components and u_i and v_i are the interpolated values of the i th approximation at the location of the observation.

The weighting factor, W , is defined by

$$W = \frac{N^2 - d^2}{N^2 + d^2} \quad (2)$$

where d is the distance between the grid point and the observation point and N is the distance at which the weight is zero.

In the iterative process of correcting the first approximation, the computer examines, or "scans" the data four times. On the first scan N is taken to be 4.7 grid lengths and it decreases to 1.5 grid lengths on the fourth scan, as shown in figure 2. This has the effect of adjusting the first approximation for the large-scale features of the circulation and later approximations for smaller and smaller features on successive scans.

The analysis program has a simple error detection test. Wind observations differing by more than 50 kt. from the first approximation are rejected on the first and second

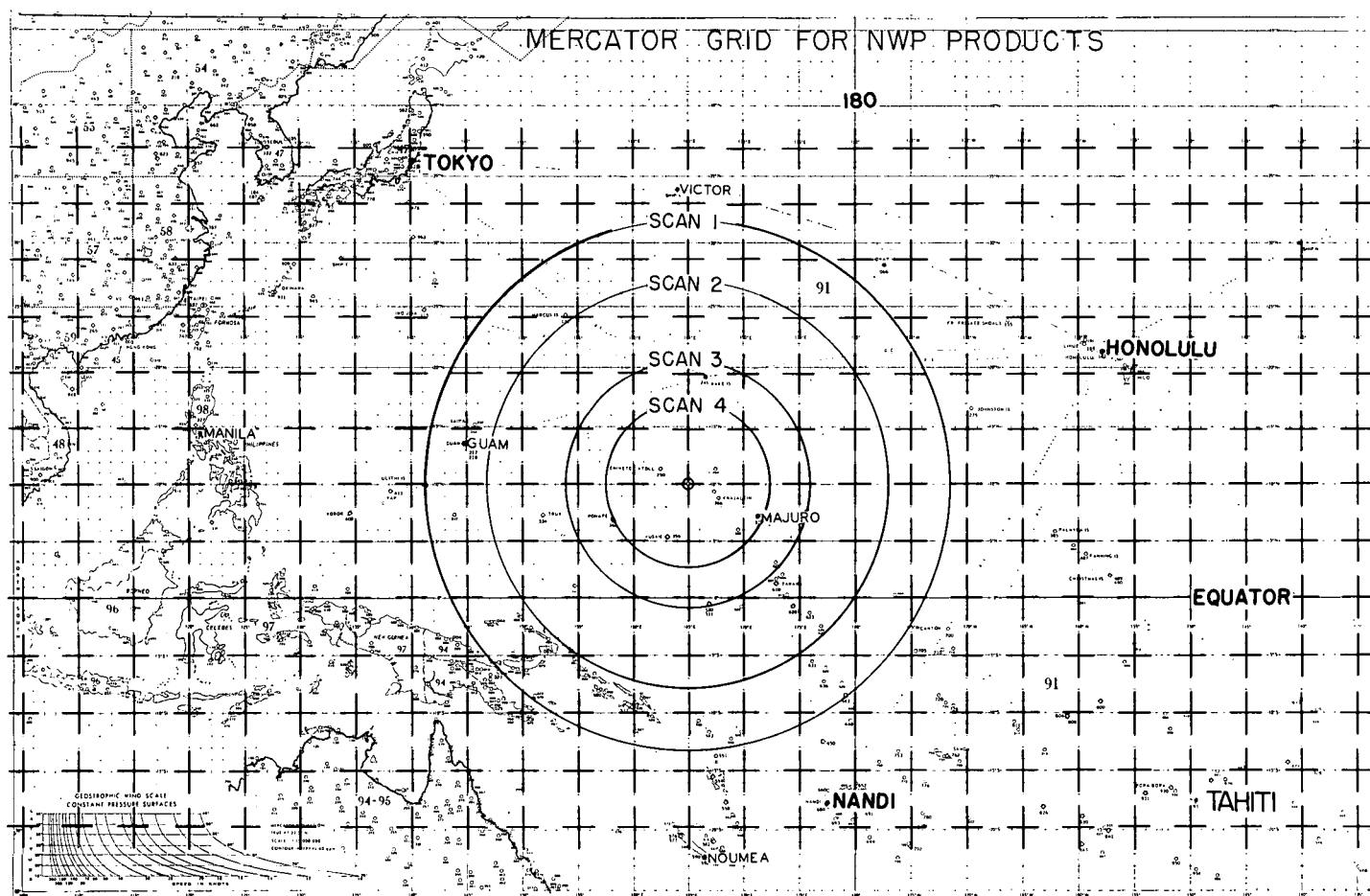


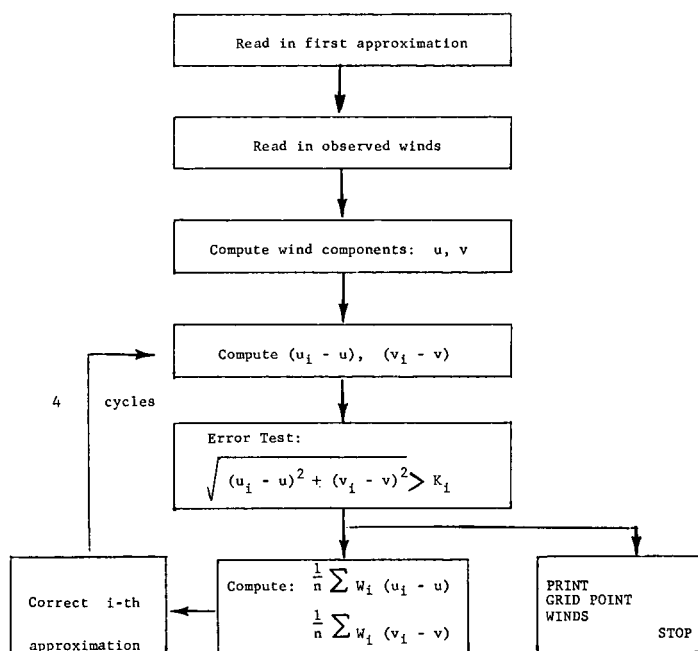
FIGURE 2.—The network of grid points used in the objective tropical analysis scheme. The areas examined on each scan are also shown.

scans, by more than 40 kt. on the third scan, and by more than 30 kt. on the fourth scan. However, the monitoring analyst may re-insert rejected data. The flow diagram of the objective analysis program is shown in figure 3. The computer print-out of the objective analysis for 200 mb. 0000 GMT June 16, 1964 is shown in figure 4.

3. EXAMPLES OF COMPUTER TROPICAL WIND ANALYSIS

A comparison of subjective wind analyses prepared by forecasters in Honolulu with objective analyses prepared by the IBM 704 computer is presented in figures 5, 6, and 7. To avoid cluttering the charts, the subjectively analyzed isotachs have been omitted.

The 300-mb. chart for 1200 GMT September 20, 1963 (fig. 5) shows good agreement over Japan among the observed winds, the subjective analysis, and the objective analysis. A closed Low is indicated by the analyst near 20° N., 165° E., whereas the objective analysis suggests a trough; the same remark applies to the Low near 21° N., 162° W. drawn by the analyst. The objective analysis indicates an anticyclonic center near 30° N., 175° W. as does the subjective. Turning next to the Southern



K_i = 50; 50; 40; 30 knots
 i = 1; 2; 3; 4
 N = 4.7; 3.6; 2.2; 1.5
 u, v = components of observed wind

FIGURE 3.—Flow diagram for tropical objective analysis program.



FIGURE 4.—Computer print-out of the objective analysis for 200 mb., 0000 GMT June 16, 1964. At each grid point the wind direction is given in tens of degrees and the wind speed in knots. The stream-gunction analysis is shown by the bands of dummy numbers. Stream-function isolines may be obtained by drawing lines along the boundaries of the bands.

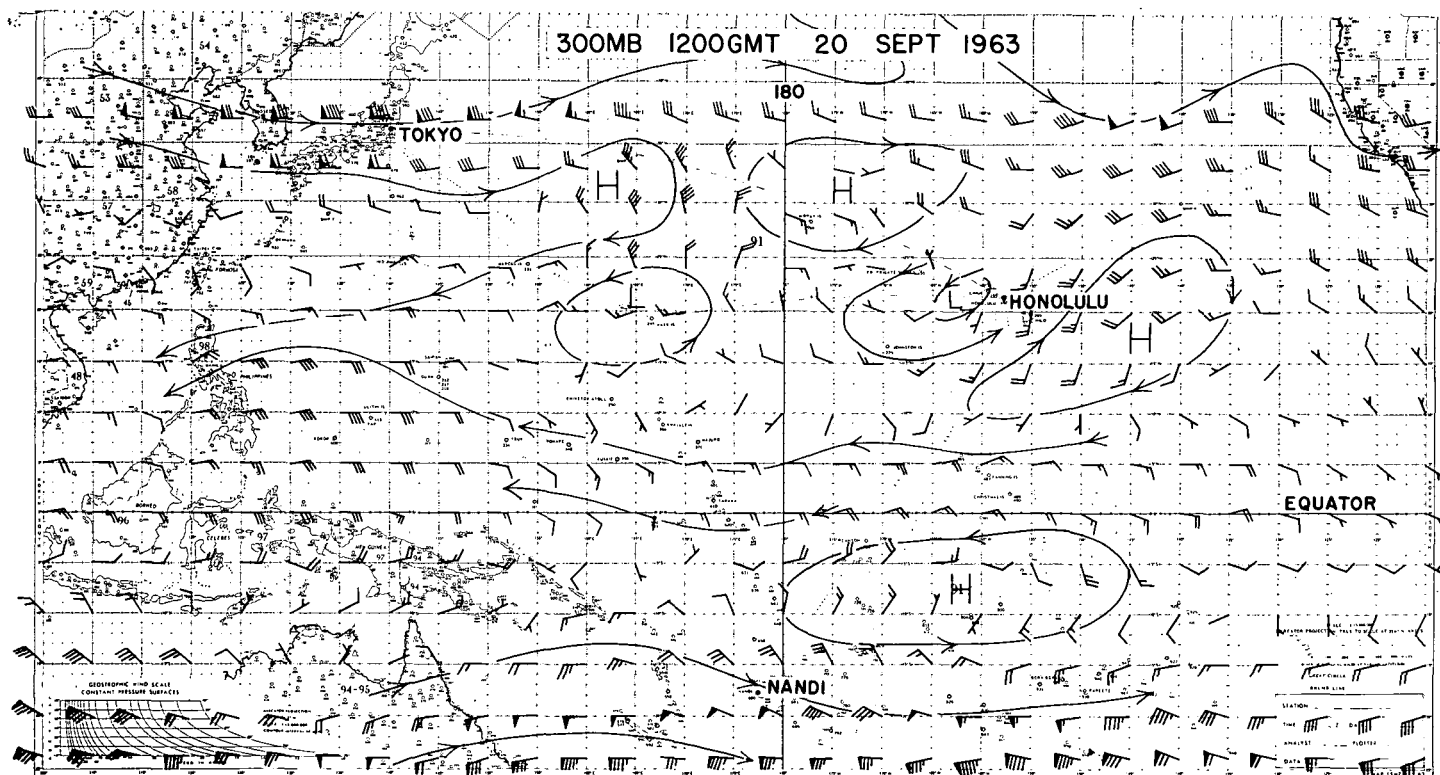


FIGURE 5.—Objective and subjective analyses of the 300-mb. chart, 1200 GMT September 20, 1963. Streamlines are from the subjective analysis; winds at uniformly spaced intervals are the objective analysis.

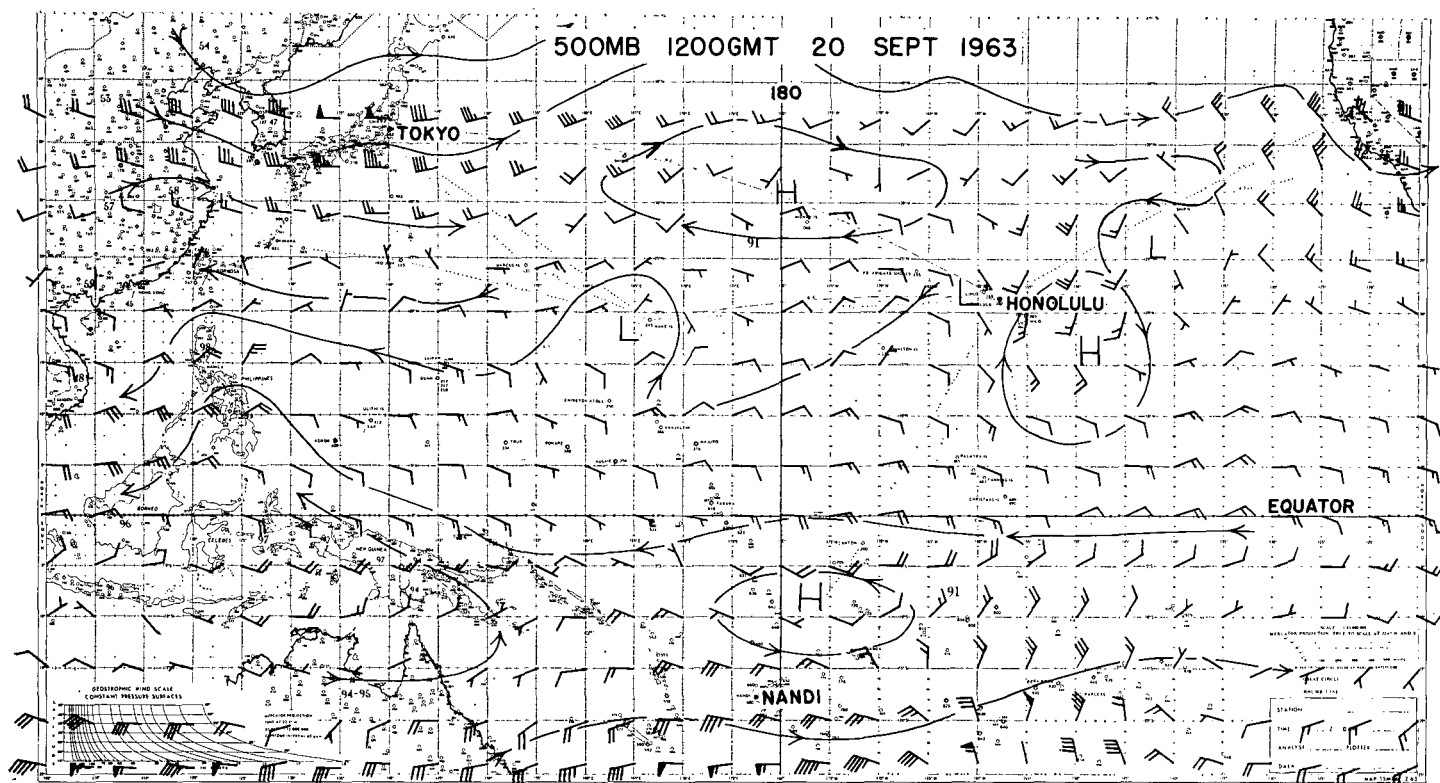


FIGURE 6.—Objective and subjective analyses of the 500-mb. chart, 1200 GMT September 20, 1963. Streamlines are from the subjective analysis; winds at uniformly spaced intervals are the objective analysis.

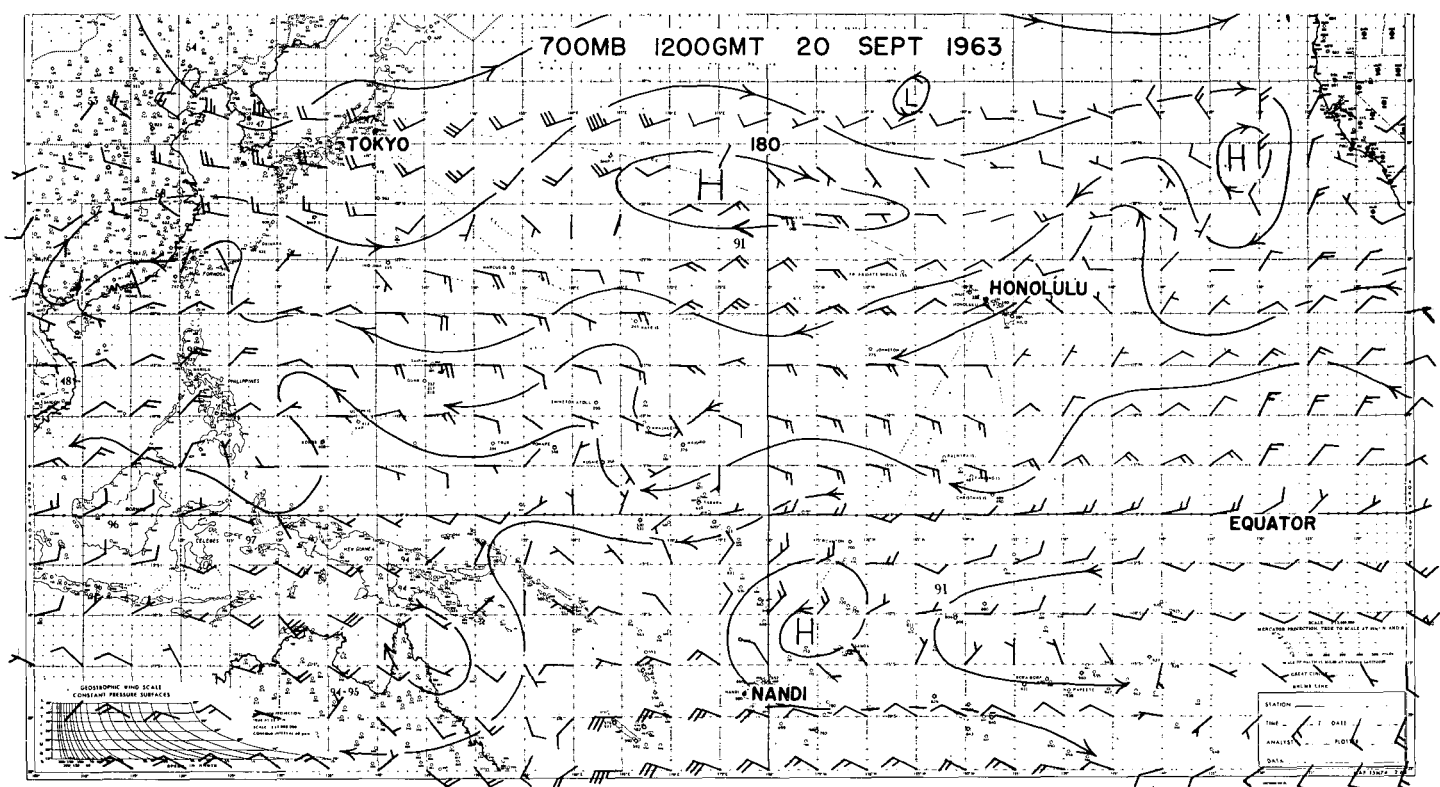


FIGURE 7.—Objective and subjective analyses of the 700-mb. chart, 1200 GMT September 20, 1963. Streamlines are from the subjective analysis; winds at uniformly spaced intervals are the objective analysis.

Hemisphere we find that both analyses agree on the location of the anticyclone near 8°S., 160°W., as well as on the associated ridge line.

The 500-mb. analysis for 1200 GMT September 20, 1963 (fig. 6) shows again the good agreement over Japan noted on the 300-mb. chart. The analyzed closed Lows near 20°N., 165°E. and 21°N., 160°W. appear in the objective analysis as troughs. The analyzed anticyclonic circulation near 32°N., 180° is not in good agreement with the computed wind in that area. There seems to be fair agreement on the location of the subtropical ridge line in the Southern Hemisphere.

Figure 7 enables us to compare the subjective and objective analyses at 700 mb. Both analyses agree on an anticyclonic circulation near 32°N., 175°E. but the ridge line extending to the east is farther north in the objective analysis. The objective analysis does not indicate the anticyclonic circulation shown by the analyst near 34°N., 132°W. The objective analysis does not indicate the trough shown in the vicinity of Wake Island (19°N., 167°E.). The objective analysis does indicate the Southern Hemisphere ridge drawn near latitude 12°S. The objective analysis cannot, of course, show the small-scale features that the analyst has tried to portray.

It is probably fair to state that, for the cases shown here, the subjective and objective analyses are in good agreement. Which is "better" is difficult to say. If forecasts derived from one type of analysis were better than those derived from another type we would say the former was "better". But tests of this kind have not been made.

4. WIND FORECASTS IN THE TROPICS

Tests by Lavoie and Weideranders [5] have shown that the subjective forecaster is hard pressed to improve on their persistence-climatology forecasts derived from

$$\begin{aligned} u_F &= (1-r_u)u_c + r_u u_p \\ v_F &= (1-r_v)v_c + r_v v_p \end{aligned} \quad (3)$$

where u and v are the west and south wind components, respectively, F refers to forecasted value, c refers to the monthly climatological value, p to persistence, and r to the lag correlation coefficient. Figure 8 shows that in 1961, for example, neither the Air Force nor Weather Bureau forecasters consistently made better forecasts for Guam than those derived from equation (3). Similar results were obtained for other tropical Pacific stations.

We have, therefore, determined the lag correlation coefficients for each grid point in our area and the computer is routinely preparing wind forecasts for the tropical Pacific based on equation (3). The meteorologist is, of course, free to adjust the computer forecasts if he so desires. That this procedure will lead to improved forecasts is quite likely. During the past two years we have been computing the persistence-climatology forecasts by

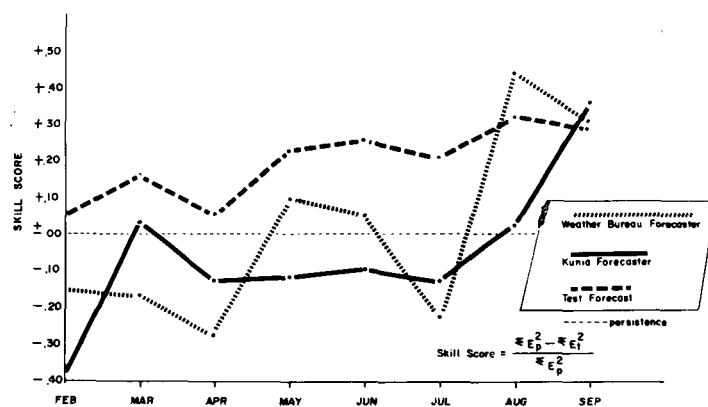


FIGURE 8.—A comparison of skill in 24-hr. wind forecasts for Guam. Most of the time the forecasts derived from equation (3) showed the highest skill.

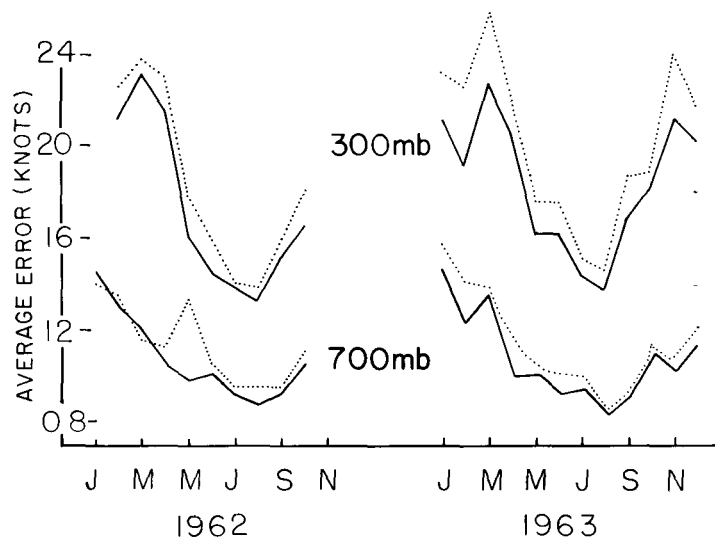


FIGURE 9.—A comparison of errors in 24-hr. wind forecasts for several tropical Pacific stations made by Honolulu forecasters (solid line) with errors in forecast derived from equation (3) (dotted line).

hand for several Pacific stations and figure 9 shows the results.

It is interesting to observe that in 1961 the persistence-climatology wind forecasts were the better ones but in 1962 and 1963 the subjective forecasts were better. The reason seems to be that the forecaster has become aware that equation (3) is a good starting point—it puts a "floor" under his score—and he deviates from it only in those cases in which he is most confident of the outcome. To put it another way, the persistence-climatology scheme by giving an acceptable initial forecast enables the forecaster to spend more time on those features of the synoptic situation to which equation (3) may not apply—typhoons, for example.

In March 1964, for example, about 1,500 flight plans were prepared from equation (3) with the aid of the com-

```

))))))))))))))))))))))))))))))))))))))))))))))))))))))))))))
FM DE 13 14W KUNIA*
KFC 14/1845*
ROUTE W774A-99 HNL-RJTY GC T/O 15/1500Z*
TO LAT/LONG ALT TYP WIND TAS GS ZD ZI TT TD TC TH MH*
BREAKERS 31 -37 08/008 403 421 030 004 0011 0074 307 308 297*
21/47 159/30 12 -3 10/020 403 420 044 006 0011 0074 307 308 297*
SOUTH KAUAI 16 -3 10/021 403 424 026 004 0014 0100 288 289 278*
LEVEL OFF 31 -37 08/008 403 411 086 013 0027 0186 287 288 277*
VANDA 31 -37 08/008 475 482 013 001 0028 0199 287 288 277*
25/53 170/0 31 -39 09/013 475 487 524 105 0132 0723 284 295 284*
26/17 171/11 31 -39 10/014 475 488 069 008 0141 0792 295 295 284*
29/11 180/0 35 -47 17/014 475 482 508 103 0244 1300 290 289 279*
31/47 170/-0 35 -46 28/044 475 487 538 116 0360 1838 286 285 280*
32/47 165/-0 35 -46 28/067 475 408 251 038 0538 2099 284 287 280*
33/35 160/-0 35 -45 28/075 475 400 256 038 0516 2355 282 282 282*
34/47 150/-0 35 -43 28/082 475 393 501 116 0633 2856 278 279 282*
35/23 142/11 35 -42 26/092 475 385 384 060 0733 3240 275 273 279*
35/41 140/11 35 -42 26/095 475 386 100 016 0748 3340 282 278 284*
KISARAZU 35 -42 26/095 475 401 024 004 0752 3364 215 223 229*
CHIGASAKI 35 -42 26/094 475 381 024 004 0756 3388 263 262 268*
YOKOTA AFB 35 -42 26/096 475 469 023 003 0759 3411 350 338 344*
WF 1ST HALF -8 2ND HALF -80 21/47 159/30 TO YOKOTA AFB -43*
=====
KFC 14/1845*
ROUTE W745A-12 JCN- HNL GC T/O 15/1500Z*
TO LAT/LONG ALT TYP WIND TAS GS ZD ZI TT TD TC TH MH*
LEVEL OFF 9 10 09/018 153 38 041 018 0018 0041 063 066 055*
17/30 168/0 9 10 09/018 204 188 059 018 0036 0099 063 065 054*
18/53 165/0 9 11 09/017 204 188 192 101 0137 0291 063 065 054*
19/35 163/30 9 10 09/018 204 188 036 31 0207 0387 065 067 056*
SWORDFISH 17 -6 10/024 245 222 046 116 0254 0693 065 068 057*
BREAKERS INT 9 9 10/017 204 187 058 019 0344 0691 089 090 079*
HONOLULU 9 9 10/017 204 187 030 010 0354 0721 089 090 079*
WF 1ST HALF -15 2ND HALF -15 17/30 168/0 TO HONOLULU -15*
=====
KFC 14/1845*
ROUTE W745A-36 JCN- HNL GC T/O 15/1500Z*
TO LAT/LONG ALT TYP WIND TAS GS ZD ZI TT TD TC TH MH*
LEVEL OFF 17 -4 07/016 183 167 077 028 0028 0077 063 065 054*
17/30 168/0 17 -4 07/016 245 229 022 005 0033 0099 063 063 052*
18/53 165/0 17 -4 08/018 245 228 192 051 0123 0291 063 064 053*
19/35 163/30 17 -5 09/020 245 227 096 025 0149 0387 065 067 056*
SWORDFISH 17 -6 10/024 245 222 046 116 0254 0693 065 068 057*
BREAKERS INT 17 -7 10/024 245 222 058 016 0310 0691 089 090 079*
HONOLULU 17 -7 10/023 245 222 030 008 0318 0721 089 090 079*
WF 1ST HALF -16 2ND HALF -20 17/30 168/0 TO HONOLULU -18*
=====
KFC 14/1845*
ROUTE W746A-99 JCN-KWJ GC T/O 15/1500Z*
TO LAT/LONG ALT TYP WIND TAS GS ZD ZI TT TD TC TH MH*
LEVEL OFF 10 8 08/018 153 169 055 020 0020 0055 255 254 244*
16/17 171/11 10 -8 08/018 204 221 044 011 0031 0099 255 254 244*
15/11 175/0 10 9 09/016 204 220 230 103 0133 0329 253 252 242*
13/35 180/0 10 9 08/014 204 218 313 126 0260 0642 251 250 240*
11/47 175/-0 10 10 07/016 204 220 314 126 0425 0956 249 249 240*
9/41 170/-0 10 9 08/022 204 227 320 125 0550 1276 248 247 238*
9/23 169/17 10 9 08/022 204 226 047 011 0603 1323 246 245 237*
KWJALIEN 10 9 08/019 204 223 100 027 0630 1423 245 244 236*
WF 1ST HALF 15 2ND HALF 22 16/17 171/11 TO KWJALIEN 17*
=====
KFC 14/1845*
ROUTE W763A-99 HNL-RPMK GC T/O 15/1500Z*
TO LAT/LONG ALT TYP WIND TAS GS ZD ZI TT TD TC TH MH*
S PORT ALLEN 16 -3 10/023 403 424 093 013 0013 0093 250 248 237*
21/47 159/30 12 -3 10/020 403 420 044 006 0011 0074 307 308 297*
LEVEL OFF 31 -37 08/010 403 414 017 003 0026 0179 278 278 267*
22/11 170/0 31 -37 08/010 475 485 506 102 0128 0685 278 278 267*
22/53 180/0 31 -37 06/004 475 478 556 110 0238 1241 274 274 265*
22/53 170/-0 35 -44 01/016 475 478 556 110 0238 1241 274 274 265*
22/17 160/-0 35 -44 35/017 475 474 555 110 0457 2349 266 266 262*
21/5 150/-0 35 -43 36/021 475 477 563 111 0608 2912 262 262 265*
19/11 140/-0 35 -42 04/006 475 480 574 112 0720 3486 259 260 261*
19/35 130/-0 35 -43 17/008 403 474 592 115 0835 4078 255 254 254*
14/35 124/-0 35 -44 12/009 475 481 366 046 0920 4444 251 250 249*
JOMALIG IS 35 -44 11/009 475 483 097 012 0932 4541 273 273 272*
ANTIPOLO 35 -44 11/008 475 482 068 008 0941 4609 263 263 262*
CLARK AFB 35 -44 11/007 475 481 051 006 0947 4660 315 315 314*
WF 1ST HALF 5 2ND HALF 2 21/47 160/41 TO CLARK AFB 3*
=====

```

FIGURE 10.—Example of computer print-out of route forecasts Johnston Island to Honolulu and Honolulu to Yokota, Clark, and Kadena. The forecast information includes temperature, wind, true air speed, ground speed, wind factors, etc. for several altitudes.

puter. These were for four different altitudes from 10,000 to 40,000 ft. and for various routes from Honolulu to the west coast of North America and to points in Asia and the Southern Hemisphere. It is planned to print out the forecasts as winds at grid points (as in fig. 4). At present the IBM 704 computer prints out route wind forecasts like the one shown in figure 10.

5. STREAM-FUNCTION ANALYSIS

In several proposed forecast models nearly non-divergent winds fields are implied. In order to accomplish this a stream function has been used to represent the winds. Endlich [6] found a stream function by using an irregular grid located at fixed observation points. It is difficult to see how to use this technique on aircraft reports for which the grid would have to vary from level to level and day to day. Rosenthal [7] hand-analyzed a wind field so as to minimize the divergence subjectively. Brown and Neilon [8] used the same methods as are de-

scribed here but discussed their results only for areas of reasonably dense data in North America.

The stream function (ψ) was analyzed as follows: Take an arbitrary value of ψ for one point on the edge. Calculate the boundary values of the stream function by integrating along the boundary line $\partial\psi/\partial s = v_n$, where s is measured along the boundary and n normal to the boundary. Distribute the difference between the starting point value of ψ and the ending point value (two values at the same point) uniformly around the edge. Solve the equation

$$\nabla^2\psi = \frac{\partial v}{\partial x} - \frac{\partial u}{\partial y} = F(x,y)$$

on the interior (F is a known function of x and y).

When daily stream-function fields were calculated, divergence errors showed up in a rather strong way. Figure 11 shows the hand-analyzed 500-mb. streamline chart for 1200 GMT May 19, 1963. Plotted at the location of the grid points are the machine-analyzed winds for that day. An inspection of the winds shows that a fairly good objective analysis was made. The amplitude of the westerly troughs and ridges at the northern boundary was not represented well because it was not reflected in the few observations along the edge and no attempt was made at manual intervention. Figure 12 shows the same case with the stream function superimposed on the computer-analyzed winds. Note that the stream function as analyzed bears little relation to the wind on the right half of the map. In fact when the vector differences between the wind derived from the stream function and the input winds are analyzed some areas of 30-kt. difference are observed.

The difficulty seems to lie in an observation (apparently a good one) located south of Tahiti. This shows a trough of the Southern Hemisphere westerlies located to the west of Tahiti. This is shown by a light southwest wind at Nandi in the Fiji Islands and a 50-kt. northwest wind at a station south of Tahiti. The machine analysis gets too large a region of outflow (though not with excessive speeds) and an insufficient region of inflow, and thus the stream function code has to seek for the required inflow, so to speak. Thus the solution that results in figure 12 is the solution we seek with a superposed point outflow region with a mean inflow all around the boundary.

Several experiments were conducted to try to correct this and at the suggestion of Mr. Edmund J. Manning we experimented with the boundary condition used in getting the stream function. The calculation of the boundary stream-function values from the normal component of the wind is simple and straightforward. Since the line integral of the tangential winds around the boundary must equal the integral of the vorticity over the interior area the wind field can also be specified by specifying the tangential component. An attempt was made to do this by successively adjusting the edge values of the stream function but this took an impractical number of scans to relax.

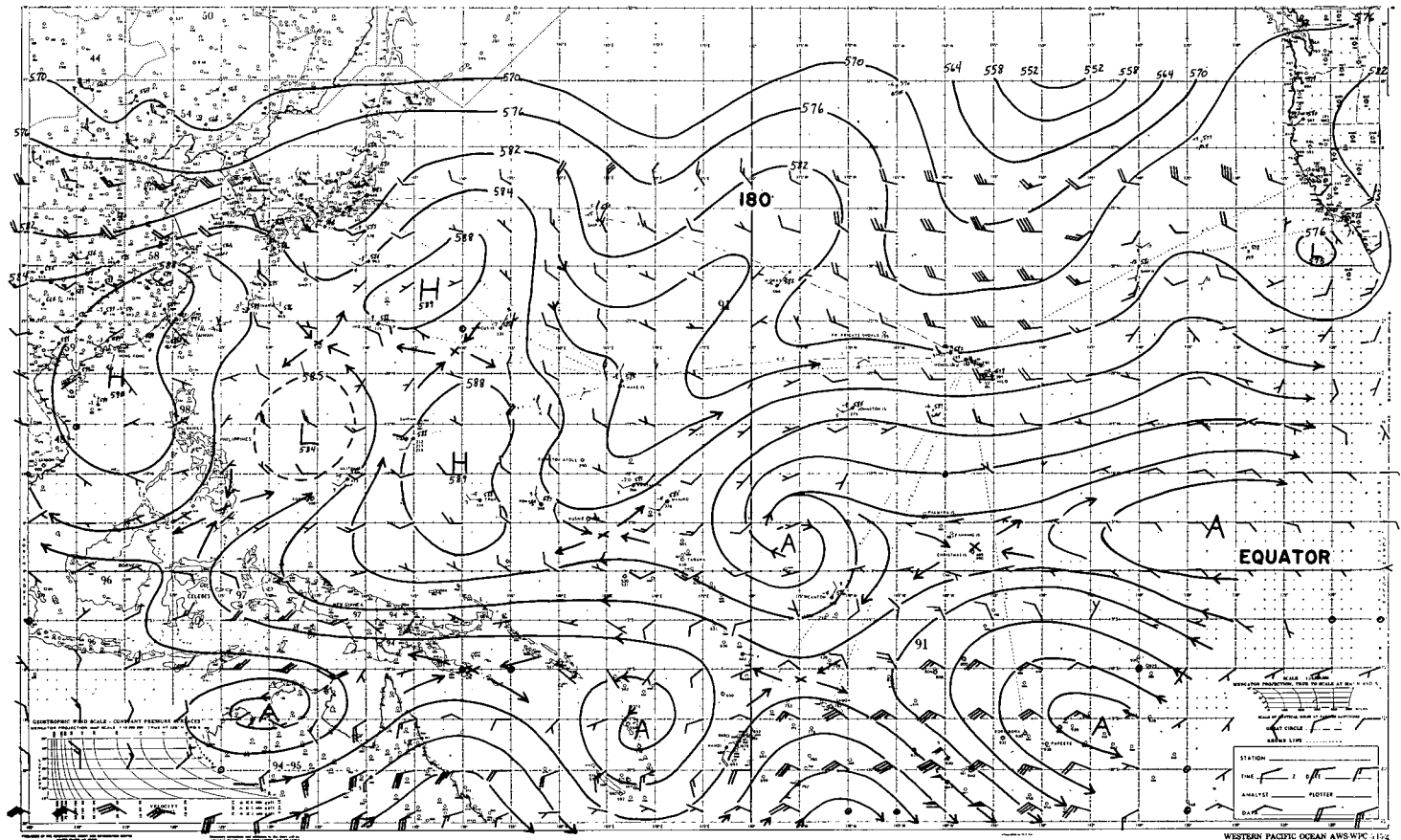


FIGURE 11.—Manual analysis for 500 mb., 1200 GMT May 19, 1963. Machine-analyzed winds are plotted at grid-point locations. Machine analysis first approximation was 70 percent persistence and 30 percent climatology.

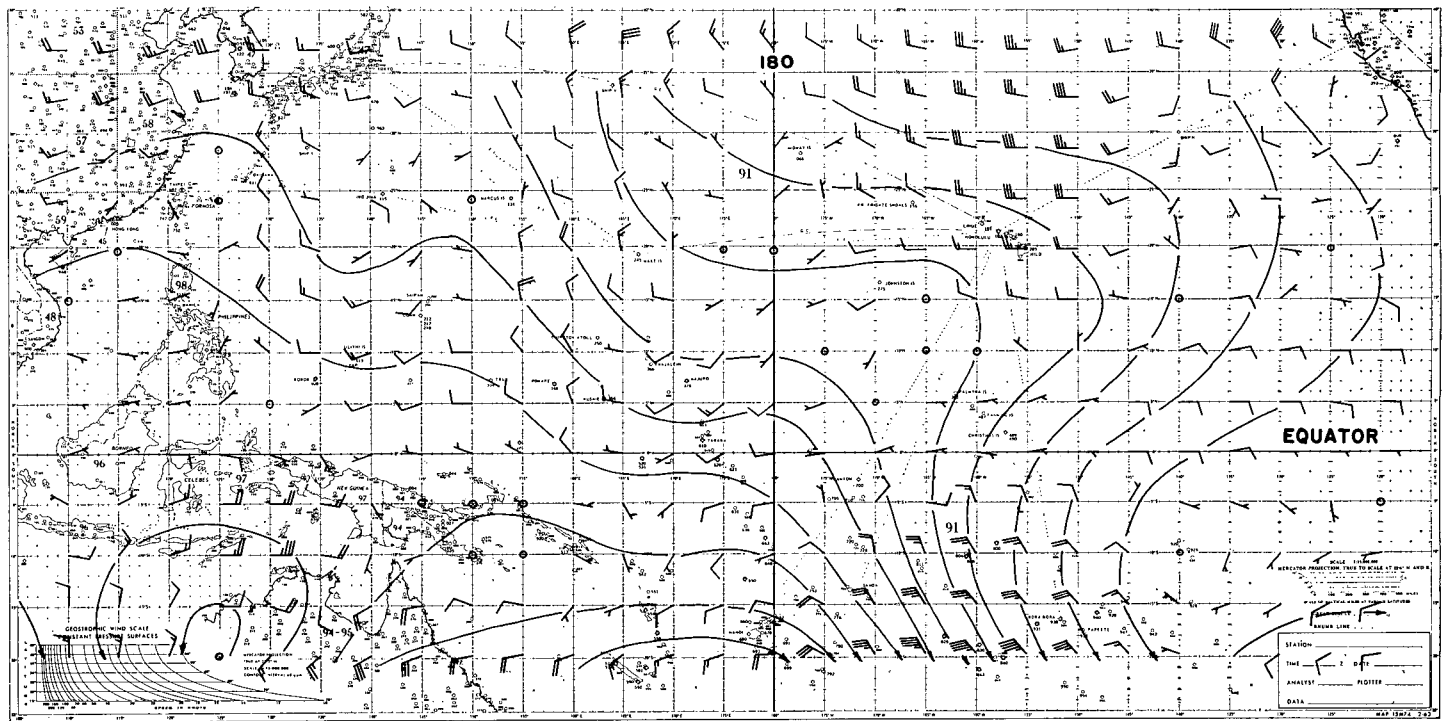


FIGURE 12.—Stream function using normal boundary conditions. Machine-analyzed winds are plotted at grid-point locations. Same case as figure 11.

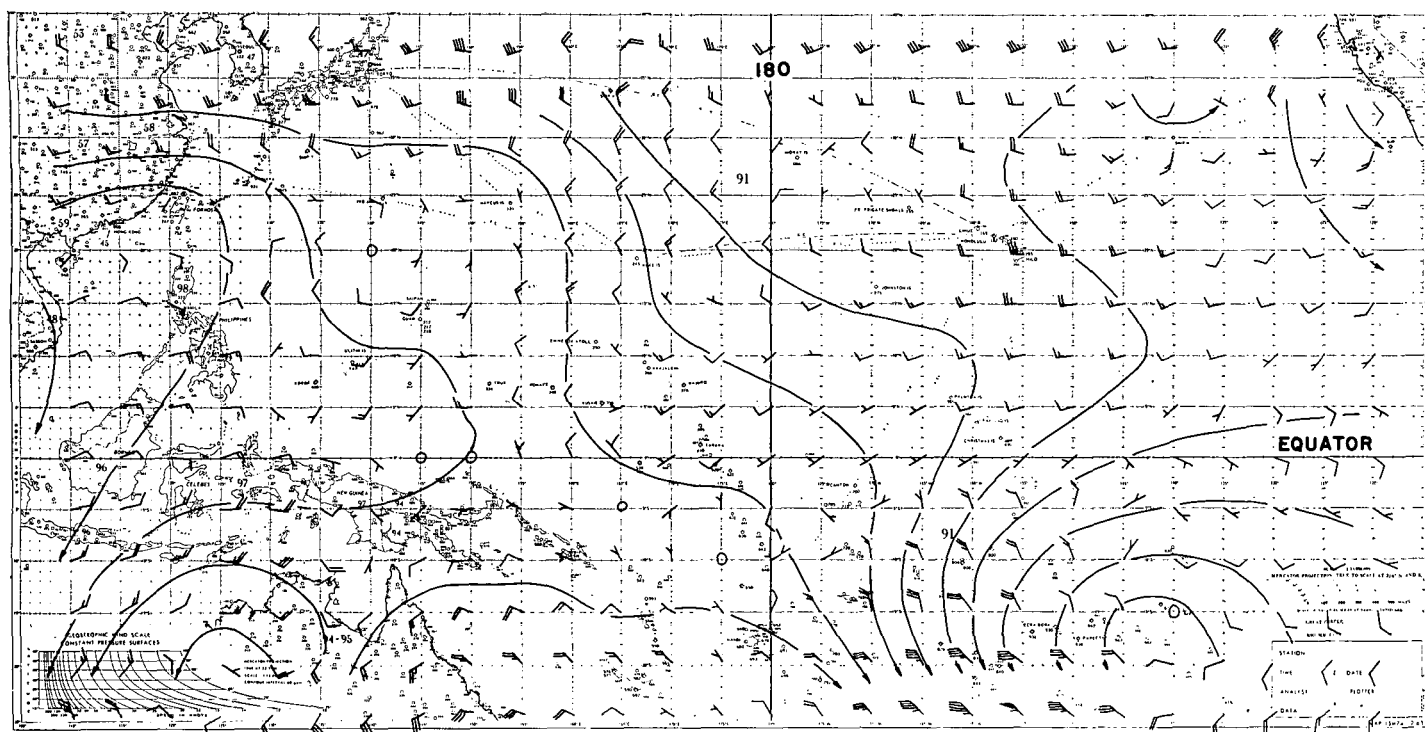


FIGURE 13.—Machine-analyzed winds and normal boundary conditions stream function for 1200 GMT May 19, 1963. First approximation was climatology.

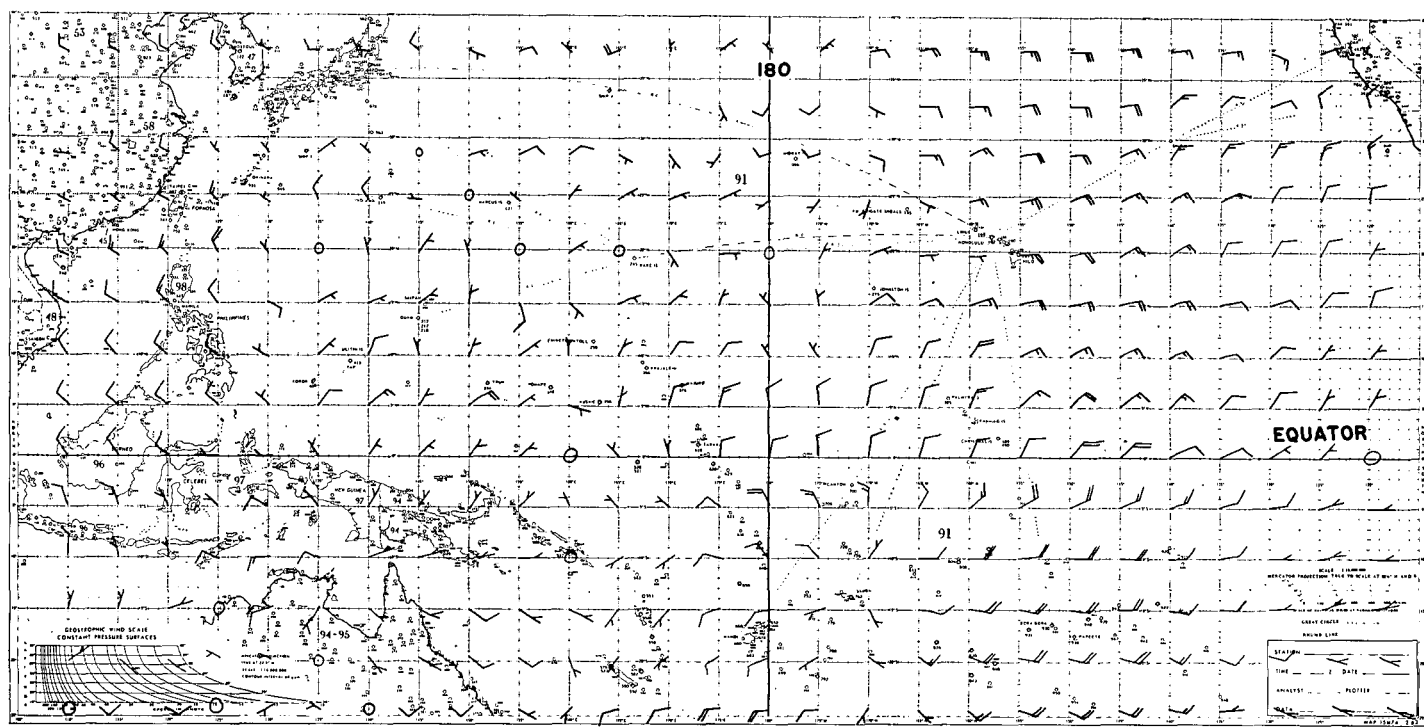


FIGURE 14.—Vector difference between stream-function winds and analyzed winds for the case in figure 13.

Another suggestion for solving this was given by Southwell [9]. By the principle of superposition of solutions the solution of

$$\nabla^2\psi = \frac{\partial v}{\partial x} - \frac{\partial u}{\partial y} \text{ (in the interior)}$$

$$\frac{\partial\psi}{\partial n} = v_s \text{ (on the boundary)}$$

should be the same as the sum of the solutions

$$\nabla^2\psi_1 = \frac{\partial v}{\partial x} - \frac{\partial u}{\partial y} \text{ (in the interior)}$$

$$\psi_1 = 0 \text{ (on the boundary)}$$

and

$$\nabla^2\psi_2 = 0 \text{ (in the interior)}$$

$$\frac{\partial\psi_2}{\partial n} = v_s - \frac{\partial\psi_1}{\partial n} \text{ (on the boundary)}$$

$$\psi = \psi_1 + \psi_2$$

Or ψ_1 can be a result of any arbitrary boundary values of ψ_1 taken perhaps from the previous day's solution and ψ_2 will be the necessary corrective to be added to satisfy the boundary conditions. The advantage of the ψ_2 field is that it is analytic on the interior. Therefore it has a complex conjugate ϕ such that

$$\frac{\partial\phi}{\partial x} = \frac{\partial\psi_2}{\partial y}$$

$$\frac{\partial\phi}{\partial y} = -\frac{\partial\psi_2}{\partial x}$$

Thus, $-\frac{\partial\phi}{\partial s} = v_s - \frac{\partial\psi_1}{\partial n}$ around the boundary and $\nabla^2\phi = 0$ in the interior. The boundary values of ϕ can be found directly and the ϕ field can be found by relaxation in the conventional way.

It is to be noted that this ϕ is not the velocity potential of the divergent component of the wind. Since the quantity ψ_2 is analytic (that is $\nabla^2\psi_2 = 0$) it is both non-divergent and irrotational and has another analytic field ϕ that is orthogonal to it.

Figure 13 is a slightly different analysis of the same case. The differences arise from the use of climatology for a first approximation instead of continuity. Figure 13 shows the new analysis and the stream function derived by using the normal component of the wind in the boundary conditions. Figure 14 shows the vector difference between the stream winds and the analyzed winds. Note that the largest errors on the boundary are tangential to the boundary, showing that the normal wind has been fitted. Small difference winds are uncertain on the boundary because of the use of uncentered differences.

Figure 15 shows the same analysis with the stream function derived by fitting the tangential component of the boundary winds. Note that the westerlies in the vicinity of the Hawaiian Islands have reappeared on the chart. Figure 16 shows the vector differences. All of the significant differences on the boundary are now normal to the edge. Internal differences have dropped in magnitude 10 to 15 kt.

The experiments described so far did not change the

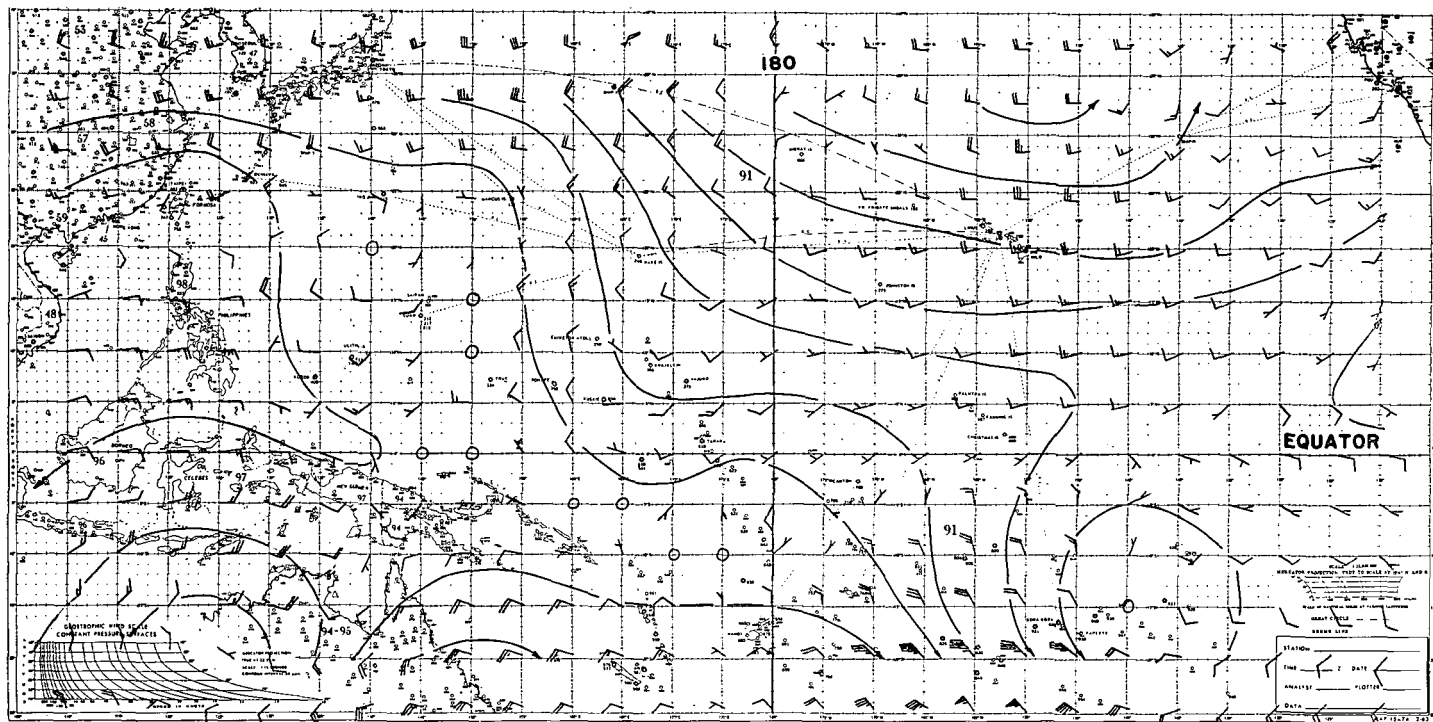


FIGURE 15.—Machine-analyzed winds and tangential boundary conditions stream function for 1200 GMT May 19, 1963. First approximation was climatology.

wind analysis, only the stream function. Experience with the method of analysis shows that it is very responsive to side conditions by adjustment of the analysis between relaxation passes. One way to get a reduction of the spurious divergence is to require the intermediate solution to be non-divergent. The result of this experiment is shown in figures 17 and 18. After the first analysis pass with the largest area of influence the stream function was derived and the analyzed winds were all replaced by the winds derived from the stream function. This procedure was repeated three times with decreasing scan radii. Figure 17 shows the resulting analysis. This technique is referred to as analysis with "feedback" from the stream-function solution. Figure 18 shows how the differences have been reduced to trivia except near the small Low off California which has not been too well represented.

This is not to say that this analysis is perfect. If figure 17 is compared with figure 11 it can be seen that there is too much flow across the equator from 150°W. to 180°. This is not derived from any data but is in response to the outflow near 20°S., 160°W. The manual analyst put in more inflow from the south near 20°S., 180° to make the analysis depict the Southern Hemisphere westerly troughs which we expect to find. The reality of the procedure will no doubt be improved by satellite observations.

Table 1 summarizes the results. The upper entry shows the root-mean-square vector difference between the observed winds and the final analysis for each level and experiment; the lower part of the table shows the

TABLE 1.—Comparison of energy measures for three stream-function methods at four levels

Height (mb.)	Normal boundary (kt.)	Tangential boundary (kt.)	Feedback (kt.)
RMS Difference Between Observations and Analysis			
700-----	7.1	7.1	7.2
500-----	7.9	7.9	7.9
300-----	8.9	8.9	8.1
200-----	6.2	6.2	6.5
RMS Difference Between Stream Function and Analysis			
700-----	5.0	4.7	2.6
500-----	10.4	7.7	4.8
300-----	14.6	11.1	6.5
200-----	16.5	17.0	7.9

root-mean-square difference between stream function and analyzed winds at all the grid points. For comparison the following are the RMS values in knots of the wind as analyzed: 700 mb., 8.3; 500 mb., 15.1; 300 mb., 30.4; 200 mb., 39.1. This can be interpreted to mean that at 500 mb. the total kinetic energy per unit area for the layer as analyzed is proportional to 225. The divergent component for the tangential boundary with feedback is proportional to 23.4 units, and the unanalyzed variability of the data is 62.5 units.

Table 1 has been included to show two things: (1) the stream function of the non-divergent part of a divergent wind field differs depending on the boundary conditions assumed, and, in general, the stream function with a

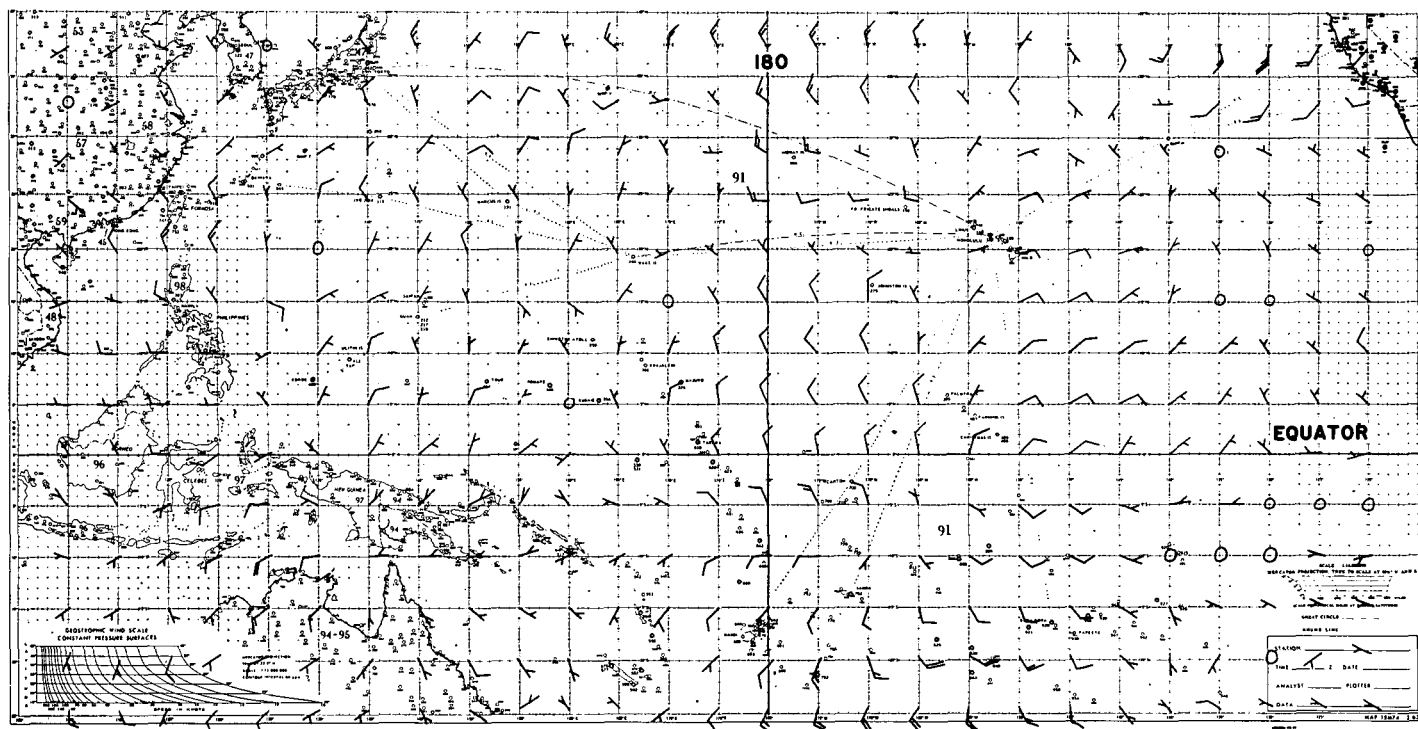


FIGURE 16.—Vector difference between stream-function winds and analyzed winds for the case in figure 15.

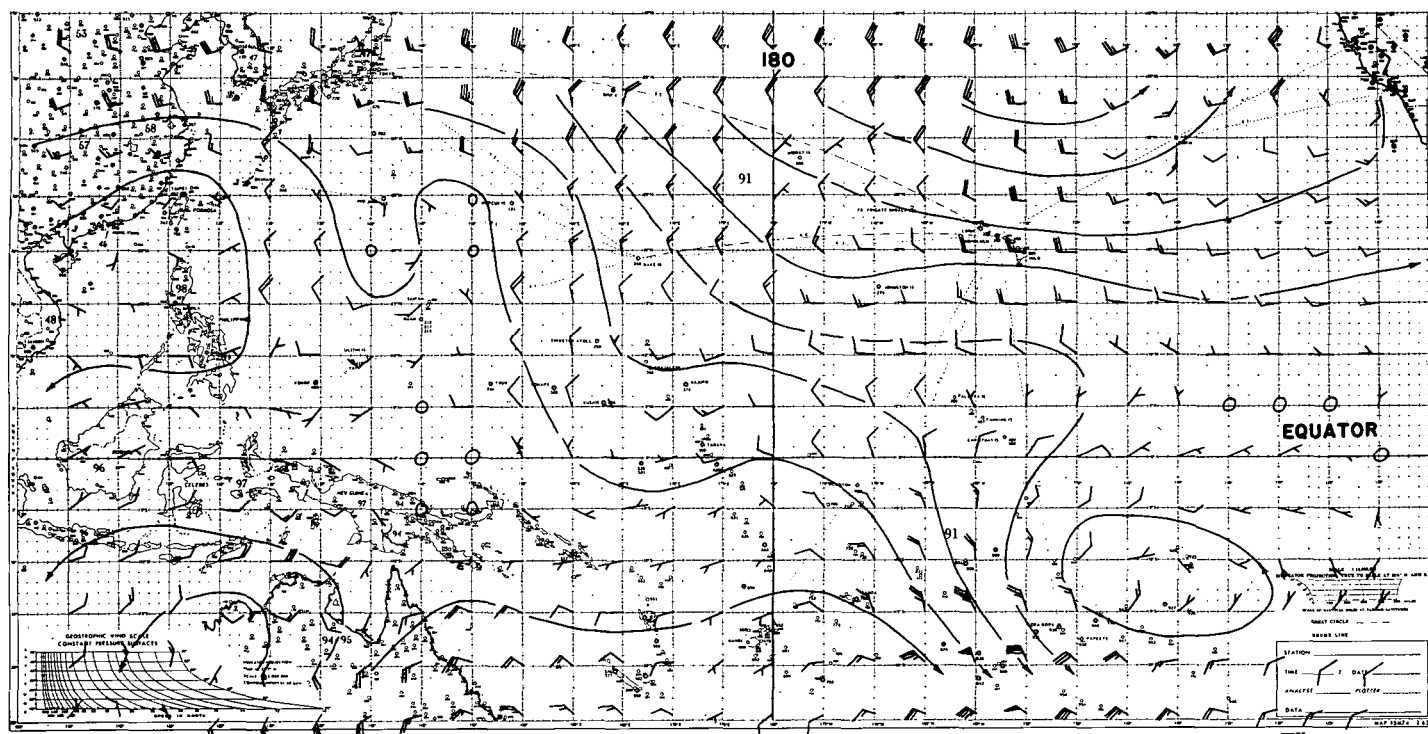


FIGURE 17.—Machine-analyzed winds and tangential boundary conditions stream function for 1200 GMT May 19, 1963. First approximation was climatology. The stream-function code has been used between analysis scans to adjust the analysis approximation to be non-divergent.

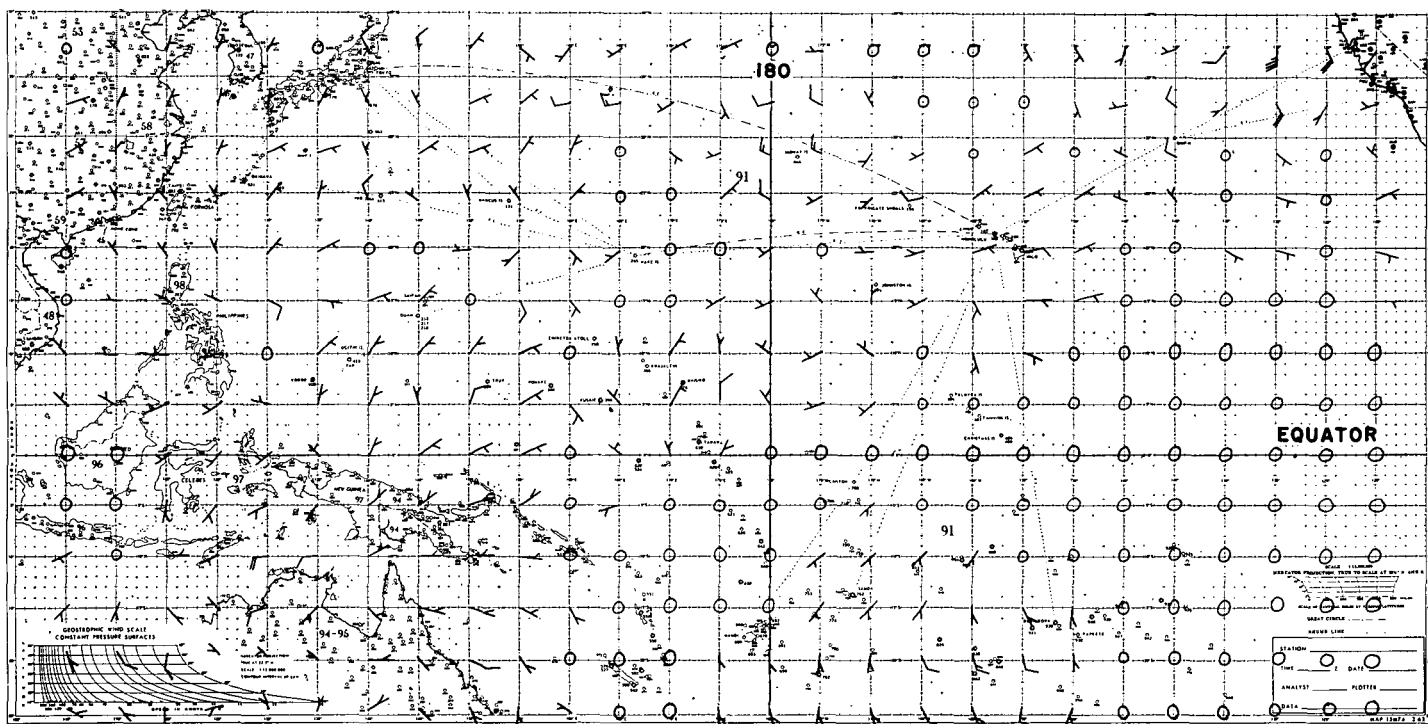


FIGURE 18.—Vector difference between stream-function winds and analyzed winds for the case in figure 17.

tangential boundary condition accounted for more of the input wind; (2) when the resulting non-divergent analysis approximation was re-analyzed the observations could be fitted as well as in the "non-feedback" analysis schemes and more of the analyzed wind field could be accounted for in the stream function.

The unanalyzed observational deviation is distributed as irregularly as the data are distributed. It includes observational error, phenomena of smaller scale than the analysis, rounding and truncation errors, the errors of the interpolating scheme, and aircraft reports moved to the nearest level and nearest time which are not truly synoptic. No attempts have been made to measure the energy levels in different wavelengths.

ACKNOWLEDGMENT

The authors wish to thank Mr. Paul R. Moore and Mr. Edmund J. Manning for their help in preparing this paper.

REFERENCES

1. L. E. Worthley, Jr., "Deviation of Geostrophic Wind from Measured Wind at 500 mb.," University of Hawaii Institute of Geophysics, Meteorology Division, *Scientific Report* No. 4, Contract No. AF 19(604)-1942, April 1959.
2. R. J. Reed, "Wind and Temperature Oscillations in the Tropical Stratosphere," *Transactions, American Geophysical Union*, vol. 43, No. 1, Mar. 1962, pp. 105-109.
3. P. Berghorsson and B. Döcs, "Numerical Weather Map Analysis," *Tellus*, vol. 7, No. 3, Aug. 1955, pp. 329-340.
4. C. P. Cressman, "An Operational Objective Analysis System," *Monthly Weather Review*, vol. 87, No. 10, Oct. 1959, pp. 367-374.
5. R. L. Lavoie and C. J. Weideranders, "Objective Wind Forecasting over the Tropical Pacific," University of Hawaii Institute of Geophysics, Meteorology Division, *Scientific Report* No. 1, Contract No. AF 19(604)-7229, AFCRL-TN-60-832, Dec. 1960.
6. R. Endlich, "Objective and Dynamical Studies of Tropical Weather Phenomena," *Quarterly Progress Report* No. 2, Stanford Research Institute, Menlo Park, Calif., 1963.
7. S. L. Rosenthal, "A Barotropic Model for Prediction in the Tropics," Third U.S.-Asian Weather Symposium, Final Report, February 1963, First Weather Wing, San Francisco, Calif.
8. J. A. Brown and J. R. Neilon, "Case Studies of Numerical Wind Analysis," *Monthly Weather Review*, vol. 89, No. 3, Mar. 1961, pp. 83-90.
9. R. V. Southwell, *Relaxation Methods in Theoretical Physics*, Oxford at the Clarendon Press, Glasgow, 1946.

[Received May 18, 1964; revised September 18, 1964]